CONTRACT SERIAL NUMBER 69169-01-SQ
CONTRACTOR: LIMPACT INDUSTRIES LTD.
REQUISITION NUMBER 23440-6-9169

High Energy Rate Compaction of R.S. Metal Powders

Final Report No. 58-10710

Limpact Industries Limited
Burnham Street
R.R. #4
Cobourg, Ontario
K9A 4J7

Attention: Mr. Robert W. Lyall, President

Submitted by:

Brenton Chen
R. T. Lassau
Materials Corrosion/Metals Investigations

October 5, 1988

55 pp

MICROMEDIA

ORTECH
INTERNATIONAL
2395 Speakman Drive
Mississauga, Ontario L5K 1B3
(416) 822-4111
Telefax (416) 823-1446

We, ORTECH Corporation, conducting business as "ORTECH International", stipulate that this document is subject to the following terms and conditions:
1. Any proposal contained herein was prepared for the consideration of the addressee only. Its contents may not be used by nor disclosed to any other party without our prior written consent.
2. Any testing, inspection or investigation performed by us will be conducted in accordance with normal professional standards. Neither we nor our employees shall be responsible for any loss or damage resulting directly or indirectly from any default, error or omission.
3. Any report, proposal or quotation prepared by us refers only to the particular material, instrument or other subject referred to in it. No representation is made that similar articles will be of like quality.
4. No report issued by us shall be published in whole or in part without our prior written consent.
5. Our name shall not be used in any way in connection with the sale, offer or advertisement of any article, process or service.
6. We reserve the right not to commence and/or continue any work until payment arrangements satisfactory to us are established.

ORTECH

High Energy Rate Compaction of R.S. Metal Powders For Limpact Industries Limited

TABLE OF CONTENTS

	Page
EXECUTIVE SUMMARY	1
1. INTRODUCTION	2
2. EXPLOSIVE COMPACTION PROCEDURE	3
2.1 Powder Preparation	
2.2 Explosive	
2.3 Cylindrical Compaction with Flyer Plate	
3. DISCUSSION	6
4. CONCLUSIONS AND RECOMMENDATIONS	9

APPENDIX A: Shock Waves
APPENDIX B: Shock Wave Compaction Geometry
APPENDIX C: Particle Effective Explosive Charge Size
APPENDIX D: Calculating Effective Explosive Charge Size

High Energy Rate Compaction of R.S. Metal Powders
For Limpact Industries Limited

EXECUTIVE SUMMARY

In a previous investigation, different High Energy Rate Compaction (HERC) processes were investigated. Explosive Compaction was one of the methods used to achieve partial consolidation of R.S. iron in this phase of the program.

High Energy Rate Compaction (HERC) processes are attractive for the consolidation of rapidly solidified materials because the particle surfaces are heated very quickly during consolidation and the heat generated is then quickly extracted into the particles resulting in only a very small temperature rise in the bulk of the material. This minimizes the degree to which the bulk material loses its rapidly solidified properties. The powders used in this phase were iron and nickel-aluminum-bronze.

Explosive compaction is at the high speed end of the HERC processes. The variable parameters for cylindrical explosive compaction are explosive burn speed, charge size, initial powder density, flyer plate and energy absorber. All the above parameters were kept constant except for charge size. The samples of iron compacted within the R values of 2.8 - 3.8 resulted in an inner and outer layered structure. The samples were above 90% of theoretical density and had consolidated areas. Two Ni-Al-Bronze samples were also compacted. The samples showed high density and had a layered phase microstructure.

1. INTRODUCTION

One of the more recent developments in metals technology has been in the area of Rapid Solidification (R.S.). This involves processes in which a molten alloy (or element) is cooled to a solid at a rate which is fast enough that the final system is not in an equilibrium state for that alloy. These techniques are supplementing alloying as a means of achieving superior materials structure and properties through microstructure control.

Structural alterations include a refined grain size (including the possibility of an amorphous state), and the addition of solutes at concentrations not possible in normal equilibrium cooling. Properties of R.S. alloys improved over conventional alloys can include hardness, superplasticity, corrosion resistance, and electrical and magnetic behaviour.

Since R.S. materials are formed from non-equilibrium processes, the products are inherently thermally unstable. The mechanics of rapid cooling usually require that at least one dimension of the product be very small (of the order of 100 μm or less). For many applications, the production of bulk, solid components from R.S. powders by some type of consolidation process is required. The usual consolidation methods considered involve the procedures developed for powder metallurgy. These techniques invariably include a sintering stage, which can cause a deterioration in the enhanced properties of the R.S. alloys.

One method being considered for the consolidation of R.S. materials is shock wave compaction. A shock wave is a disturbance which passes through a sample and causes an almost instantaneous change in the pressure-volume state of the material in the vicinity of the disturbance. Shock waves are described in Appendix A of this report.

Shock wave compaction is a unique method of compacting a powder sample. It has the potential of selectively treating (and possibly melting) the outside of the powder particles (1), a feature which is desirable in the bonding of thermally unstable materials. There are, however, a number of difficulties to be overcome before this technique could become practical. Cylindrical compaction, which must be carried out using explosives, has fewer equipment requirements, but tends to generate a structurally unsound region along the centre of the sample. Because of its simplicity and lower equipment costs, cylindrical compaction was used for the trials carried out in this project.

The R.S. materials that were used for these compaction trials were water atomized iron and nickel-aluminum-bronze powders.

This final report summarizes the work carried out under contract to Limpact Industries Limited. The cylindrical explosive compaction method is described in Section 2. An overall discussion of the sample properties is included in Section 3, with conclusions and recommendations in Section 4. In addition, four appendices are attached to provide details of theories concerned with explosive phenomena.

2. EXPLOSIVE COMPACTION PROCEDURES

Explosive compaction trials were carried out using the cylindrical geometry shown in Figure 3. Shock wave propagation in this geometry is described in detail in Appendix B. The procedures for the compaction trials are described below. Also described are the procedures involved in preparing the powders for use in the compaction samples.

2.1 Powder Preparation

The materials chosen for HERC were iron and nickel-aluminum-bronze. One of the more important features of HERC is the expectation of particle surface heating, and possibly melting, during the passage of the shock wave (Appendix C).

The iron powder used was water atomized Hoeganaes 1000, and the water atomized nickel-aluminum-bronze powder had a nominal composition of 5.8% nickel, 6.4% iron, 0.64% manganese, 9.3% aluminum and 77.86% copper.

Both powders were reduced in hydrogen before being sealed into the sample tubes. This was done to remove oxide layers which tend to form on fine metal powders. Such oxide layers can inhibit bonding between the powders on compaction. The reducing schedules are listed in Table I.

The powders were subjected to sieve analysis to determine their size distribution. The size distributions are listed in Table II. The microhardnesses are listed in Table III. Photographs of the microstructures are shown in Figures 1 and 2.

2.2 Explosive

The explosive used in this project was Amatol. The properties of the explosive are listed in Table IV. The procedure for calculating the effective charge size is given in Appendix D.

Amatol is a mixture of ammonium nitrate and trinitrotoluene. This explosive is characterized by high density, high energy density and fast burn speed. It comes in a particulate form.

2.3 Cylindrical Compaction with Flyer Plate

The compaction trials used the geometry shown in Figure 3. There are a number of variables in this geometry, and many of these were examined in a previous investigation (2). The optimum parameters were selected (2) for all the trials in this phase. The only parameter that was varied was the charge size.

The basic configuration is a cylindrical tube containing the powder to be compacted and a 1.59 cm (5/8") mandrel sealed at both ends. This tube is placed inside a second tub e (flyer plate) with a gap of approximately 16 mm (1/16") between the tubes. This assembly is then placed vertically inside a larger plastic (PVC) tube. The region between them is then filled with Amatol. The explosive is detonated from the top. The detonation front progresses from the top of the sample to the bottom. As the burn progresses, combustion product gases cause a rapid pressure increase which compresses the flyer plate, allowing it to accelerate to a high velocity. It impacts on the sample tube, creating a sharp shock front which compresses the sample tube, compacting the powder. Shock waves are described in Appendix A.

The tubes used to contain the powder were cut from lengths of extruded mild steel 22.2 mm I.D. and 25.4 mm O.D. (7/8" and 1"). Sample tube lengths were 178 mm (7") with 25.4 mm (1") long steel plugs silver soldered into each end to seal the powder in the tube. Samples were weighed before and after filling to determine the powder mass, and the

pre-compaction density was determined by dividing this mass by the known sample volume.

The final densities and hardnesses of all the samples were measured after compaction. The results of these measurements are shown in Tables V and VI. In these tables, R is the ratio of explosive charge mass to flyer plate mass. The variable R determines the amount of energy transferred from the explosive to the sample. All sample densities were measured by fluid displacement, using ethanol.

3. DISCUSSION

In an earlier phase (2), explosive compaction was investigated, with explosive burn speeds up to 5 km/s, to find the optimum conditions for the compaction of metal powders. The parameters included burn speed, charge size, initial powder density, and the effects of flyer plates and energy absorbers in the sample. After careful analysis, the optimum parameters were chosen and powder samples were compacted radially. Although the samples showed high density values, they were not properly bonded. Sintering of explosively compacted samples was found to be impractical, because of large elongations and cracking caused by high levels of residual stress. Compaction trials, using a linear geometry, were of limited success. It was concluded that explosive compaction of metal powders would not be a feasible process unless a number of problems were solved, problems that included addressing bonding between particles, the tendency for cracking and for the presence of high levels of residual stresses in the samples.

In this, the second phase of the program, the only parameter to be varied was the charge size. All other parameters for cylindrical

explosive compaction, such as explosive burn speed, initial powder density, flyer plate and energy absorber geometry, were held constant. Recognizing that the application of explosive compaction is very alloy dependent, the consolidation characteristics of pure iron were to be studied under the following conditions.

- A non-tapered mandrel (diameter 1.6 cm) was used along the central axis of the powder sample to reduce the effect of the convergence of the shock pulse.

- The material used to house the iron powder and the mandrel was a seamless 20 gauge (2.5 cm O.D.) mild steel tube.

- A flyer plate external to the sample was used to increase the shock wave pressure without increasing the energy of the pulse.

- External PVC jackets were used to house the explosive (AMATOL) of varying radial dimensions that provided a ratio of explosive mass to tube mass of R = 1 to R = 5 over the range of experiments.

- Iron powder was reduced in hydrogen before being sealed into the sample tubes and the powder was not precompacted.

Tables V and VI and figures 4 - 9 are summaries of the results obtained for density measurements and bonding characteristics of iron and nickel-aluminum-bronze rapidly solidified powders.

Table V summarizes the densities obtained at various locations on compacted iron product for four different ratios of explosive mass to sample tube mass. In addition, hardness values were measured in positions labelled "top, middle, bottom" referenced to the conical end of the energy absorbing mandrel as the "top".

For R = 1 and 2, the compacted densities were higher than for R = 3 and 4, primarily because of the inclusion of voids in the consolidated iron product at the higher R values. Figure 4 shows the microstructure of the compacted product formed at R = 1. Consolidation was not evident, and above the mandrel the region was structurally damaged. The variation in density from top to bottom (Figure 10) shows that the consolidation mechanism, as it depends on the shock wave, is a function of the system geometry.

The hardness measurements support the observed absence of consolidation in this product.

Consolidation was achieved at higher R values. Figure 5 shows the layered structure that occurred for R = 2.8 which may be a result of sharpening of the shock wave as it passes through the powder(3). The most promising bonding results were obtained at mid-thickness where the shock wave had sharpened, but where recoil waves had minimum effects.

Figure 6 shows consolidated powders at R = 3.8. The inclusion of voids is now apparent, in agreement with the decrease in measured density.

Consolidation attempts at an explosive mass to sample tube mass ratio of 5.2 resulted in a product that was quite similar to R = 3.8, with the exception that the "apparent" void content were higher (Figure 7). The conclusion, therefore, was that the optimum charge size had been spanned and, indeed, peaked between R = 2.8 and R = 5.2 for the iron powder.

Table VI and Figures 8 and 9 represent the results of the consolidation of the water atomized powder nickel-aluminum-bronze.

For R = 2.8 and 5.2, the products showed some evidence of consolidation, but under optical magnification, the microstructures (Figures 8 and 9) appeared quite complicated with at least three distinct phases showing. The phase furthest from the region of the mandrel showed some evidence of maintaining the original RS microstructure. Extensive electron optical work would be required to determine the nature and composition of these phases, but such studies were postponed for a subsequent phase, continuing this program.

4. CONCLUSIONS AND RECOMMENDATIONS

This report describes the investigation of charge size on the High Energy Rate Compaction (HERC) of metal powders. Conclusions can be summarized as follows.

- Precompaction of the sample powder has the effect of decreasing the size of the central channel, but does not affect the final density or aid in particle bonding.

- The use of a flyer plate sharpens up the shock front, effectively increasing the shock pressure for a given shock energy. This results in an increase in the final density.

- Considerable evidence has been provided for bonding or particle surface melting for iron powder with explosive mass to sample tube mass ratios between 2.8 and 5.2. Bonding was also evident in the nickel-aluminum-bronze RS product, but microstructural

complications denied easy interpretation of the data. It is, however, quite apparent that the methodology is alloy dependent.

In conjunction with the results of an earlier investigation involving a number of parameters affecting powder consolidation, the progress to date, in terms of the total data collected, affords an excellent opportunity to remain at the forefront of this technology in the area of methodology. Specific items that need to be addressed now are:

- system geometry studies that might incorporate sintered centre rods for improved energy absorption to reduce the after shocks that tend to stress and damage the consolidated product;

- compilation of current literature data comparing peak stress and energy for melting different alloys which would serve as data for studies on models that could predict energies and pressures;

- studies related to the dependence of consolidation characteristics on particle size, perhaps in the region of 100 μm.

Considering the potential that HERC processing has, the continuation of this work is highly recommended with a specific industrial product as the end objective.

for B. Chen
Project Technologist
Metals & Corrosion Technologies

R. T. Lassau
Manager
Metals & Corrosion Technologies

TABLE I

POWDER REDUCTION SCHEDULE*

Iron	720°C	for 1 hour
	735°C	for 20 minutes
Al-Bronze	300°C	for 75 minutes

*All powders were reduced in hydrogen at the indicated temperatures prior to compaction.

TABLE II

PARTICLE SIZE DISTRIBUTION
(as a percentage)

Size Range (μm)	Iron	Al-Bronze	Size Range (μm)
+149	13.01		
-149/+104	17.98		
-104/+74	20.46	2.3	+850
-74/+62	9.26	24.0	-85/+149
-62/+44	12.81	53.7	-149/+44
-44	26.48	20.0	-44

TABLE III

POWDER HARDNESS

Material	Hardness (VHN)
Iron	80.6
Al-Bronze	288.0

TABLE IV

PROPERTIES OF EXPLOSIVE

Explosive	Heat of Explosion (kJ/kg)	Detonation Velocity (km/sec.)	Density (g/cm^3)
Amatol	4100	5.2	1.6

TABLE V

AS COMPACTED IRON SAMPLES

Sample	#1	#2	#3	#4	Consolidated Piece
R*	1.0	2.8	3.8	5.2	
Initial Density (% Theoretical)	59.5	59.8	59.6	59.6	
Final Density (% Theoretical Avg.)	96.3	96.2	92.4	91.0	99.8
Top	101.2	99.4	93.6	93.7	
Middle	96.6	96.1	92.2	91.0	
Bottom	91.2	93.1	88.4	89.2	
Energy Absorbing Mandrel	YES	YES	YES	YES	
Flyer Plate	YES	YES	YES	YES	
Explosive	Amatol	Amatol	Amatol	Amatol	
Hardness					
VHN (avg.)	174	226	275	275	281
$H(R_b)$ (avg.)	87	98	-	-	-
$H(R_c)$ (avg.)	-	-	26	26	29

*R is the ratio of explosive mass to sample tube mass.

TABLE VI

AS COMPACTED Al-BRONZE SAMPLES

Sample		#1	#2
R*		2.8	5.2
Initial Density (% Theoretical)		34.3	34.5
Final Density (% Theoretical Avg.)		88.0	90.2
Top		91.0	90.0
Middle		90.5	87.7
Bottom		82.4	92.8
Energy Absorbing Mandrel		YES	YES
Flyer Plate		YES	YES
Explosive		Amatol	Amatol
Hardness (VHN) HR_C			
• Near Mandrel	Top	(441),45	(362),37
	Middle	(386),39	(454),46
• Outer Layer	Top	(412),42	(386),39
	Middle	(429),43	(454),46

*R is the ratio of explosive mass to sample tube mass.

BIBLIOGRAPHY

(1) Gourdin, W. H., J. App. Phys., 55, 1984, pp 172-181.

(2) Sullivan, J. D., Shimizu, H., "High Energy Rate Compaction of R.S. Metal Powders", ORF Report No. 58-10376 to Limpact Industries Limited, January 1986.

(3) Gourdin, W. H., Progress In Materials Science, 30, 1986, pp 39-80.

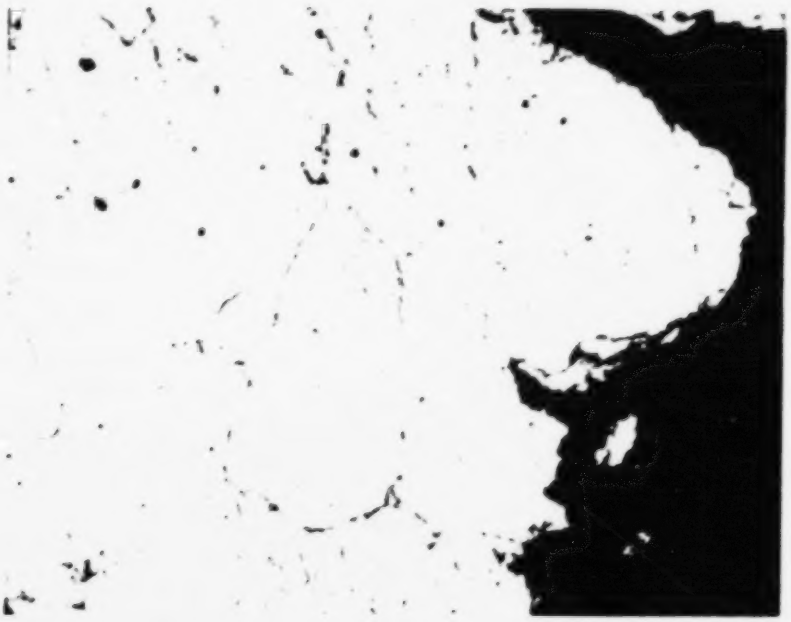

FIGURE 1: Microstructure of the iron powder.
MAG.: X1600.

FIGURE 2: Microstructure of the nickel-aluminium-bronze powder.
MAG.: X1250.

Figure 3

Cylindrical Sample Geometry with Central Energy Absorbing Mandrel and Outer Tube Flyer Plate

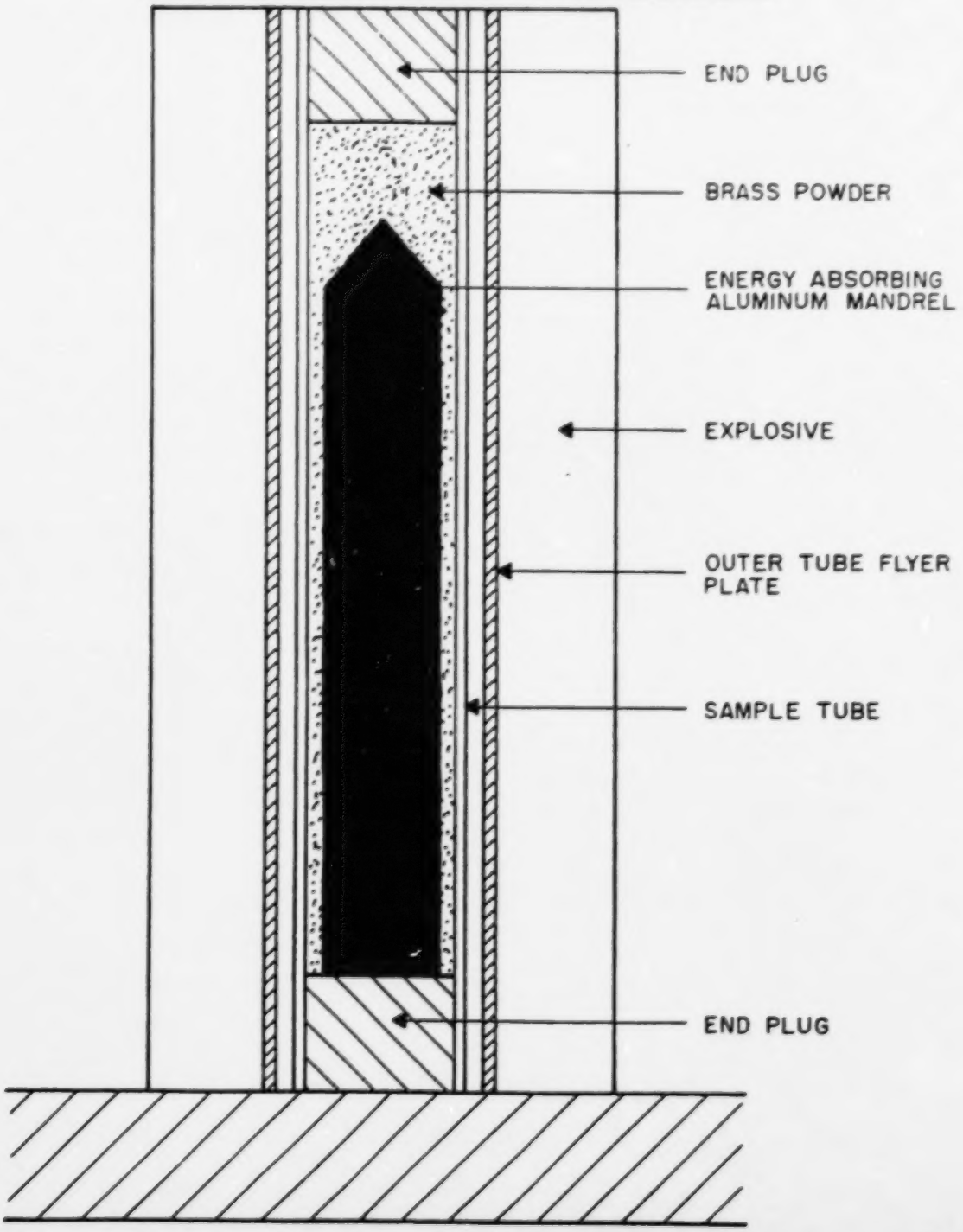

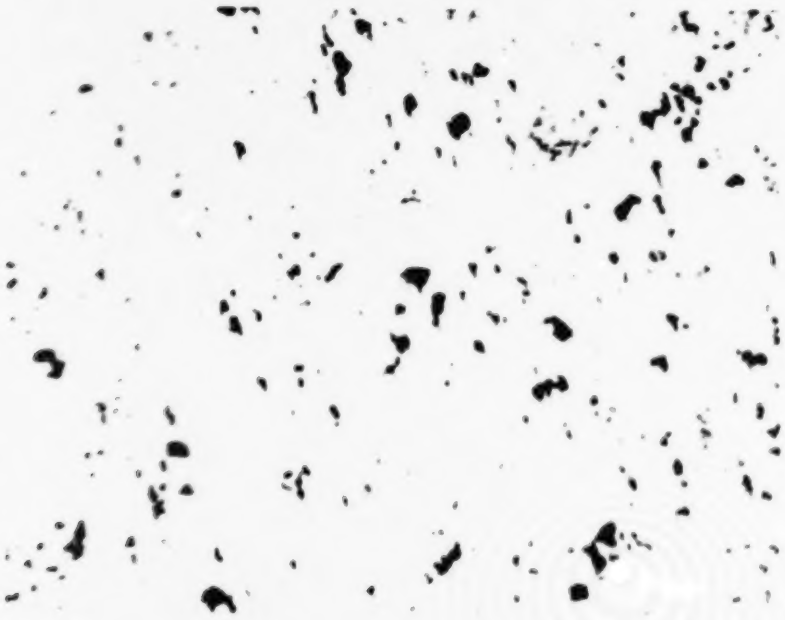

FIGURE 4: Unetched surface of a compacted iron sample.
R= 1.0
MAG.: X125.

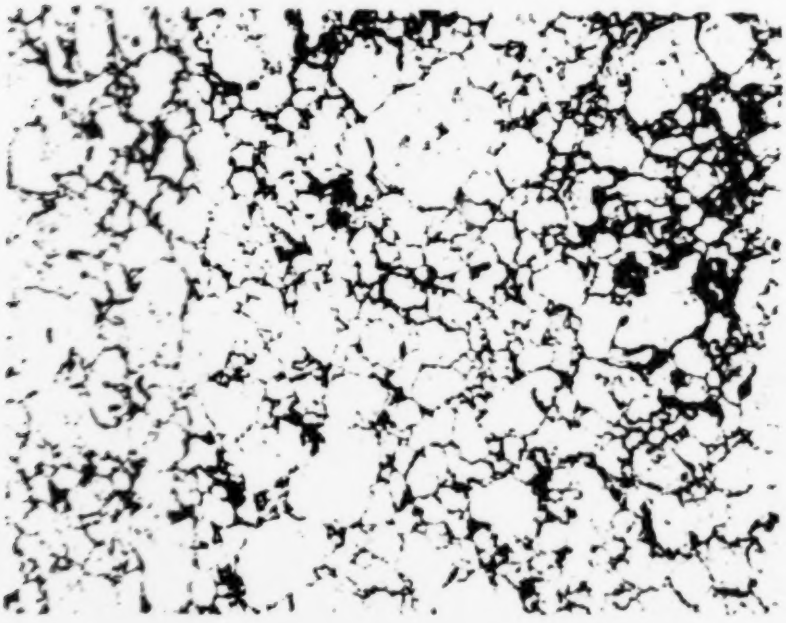

FIGURE 4a: Microstructure of the compacted iron, R = 1.0.
MAG.: X125.

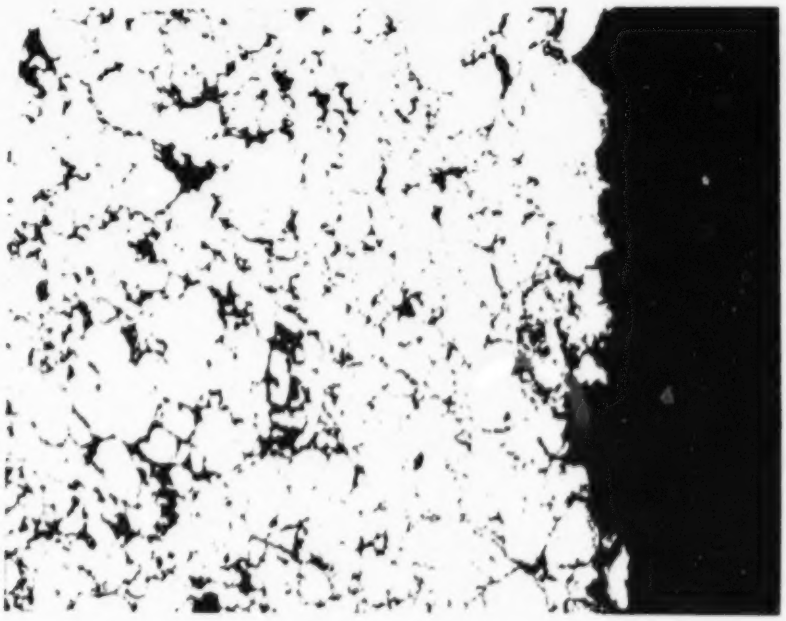

FIGURE 4b: Microstructure of R = 1.0,(beside the mandrel) showing there is NO layered formation.
MAG.: X125.

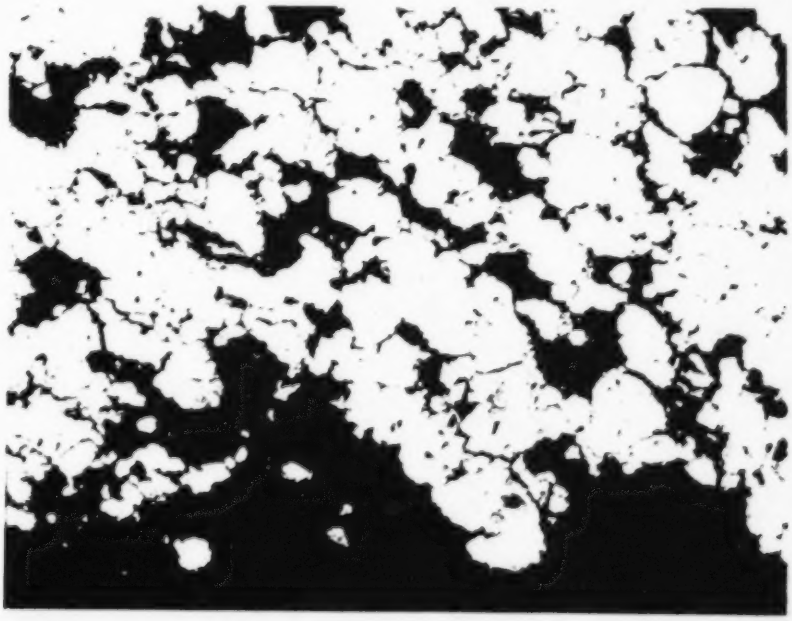

FIGURE 4c: Microstructure of R = 1.0 above the mandrel. Mach stem beginning to form.
MAG.: X125.

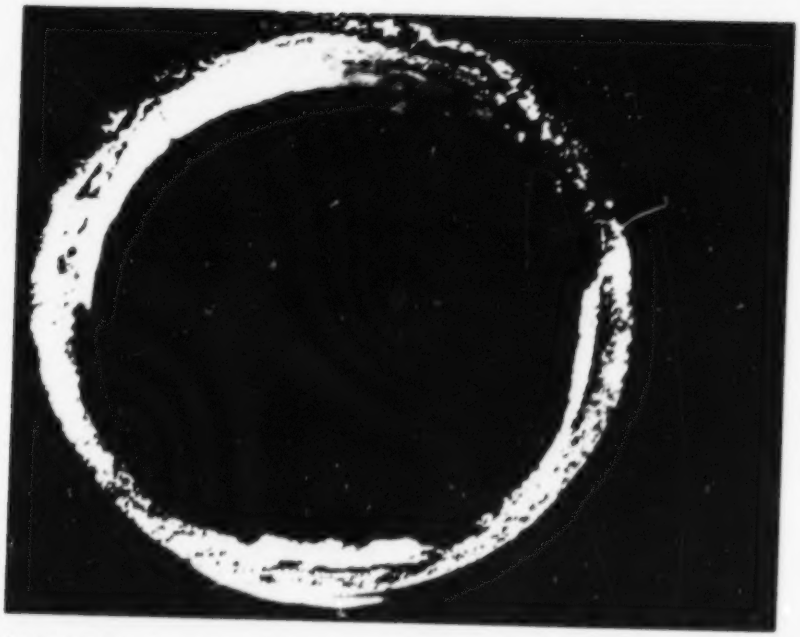

FIGURE 5: Section of compacted iron sample (mandrel removed) showing layered formation. R = 2.8.
MAG.: X 5.

FIGURE 5a: Unetched surface of compacted iron sample, R= 2.8.
MAG.: x 500.

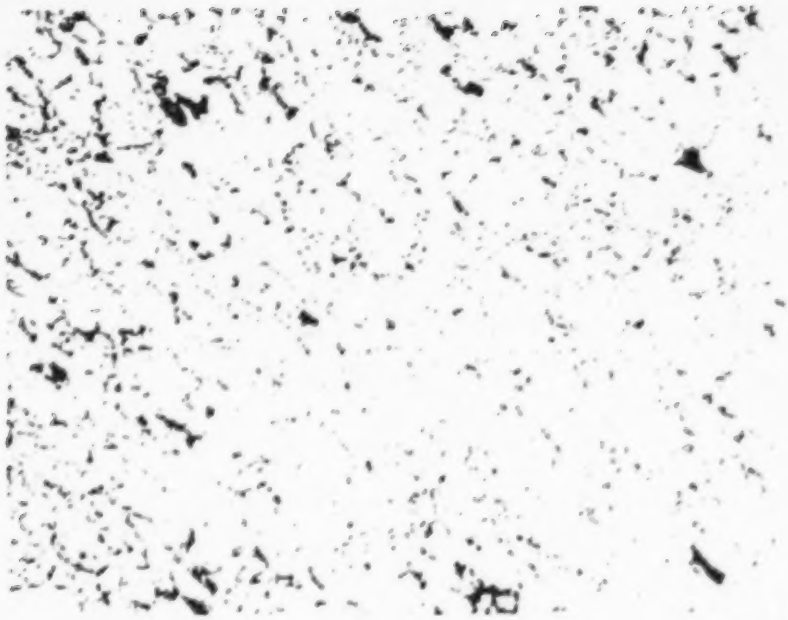

FIGURE 5b: Microstructure of iron sample, R = 2.8.
MAG.: X 100.

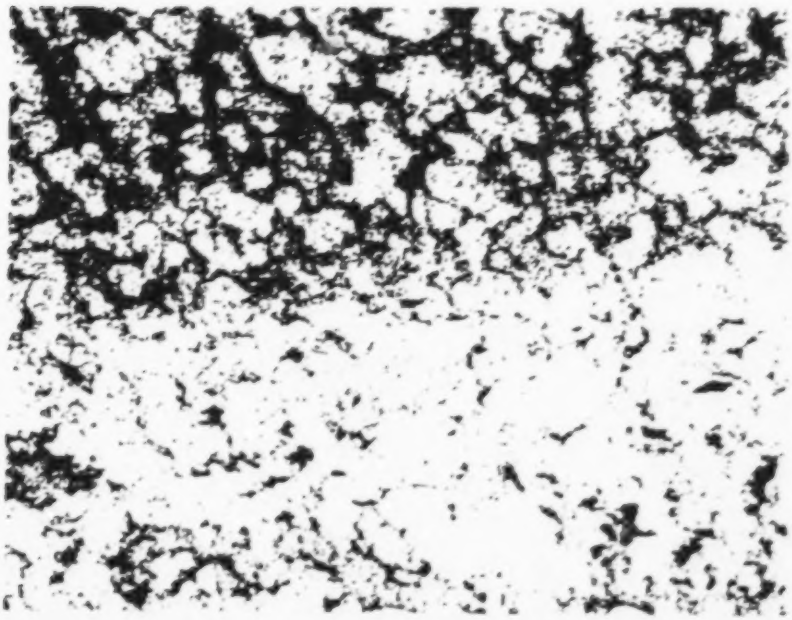

FIGURE 5c: Microstructure of the layered formation of R = 2.8.
Top is outer layer, bottom is inner layer.
MAG.: X 100.

FIGURE 6: Unetched section of the top piece (no mandrel) of the iron sample compacted at R= 3.8, showing the mach stem.
MAG.: X 21.

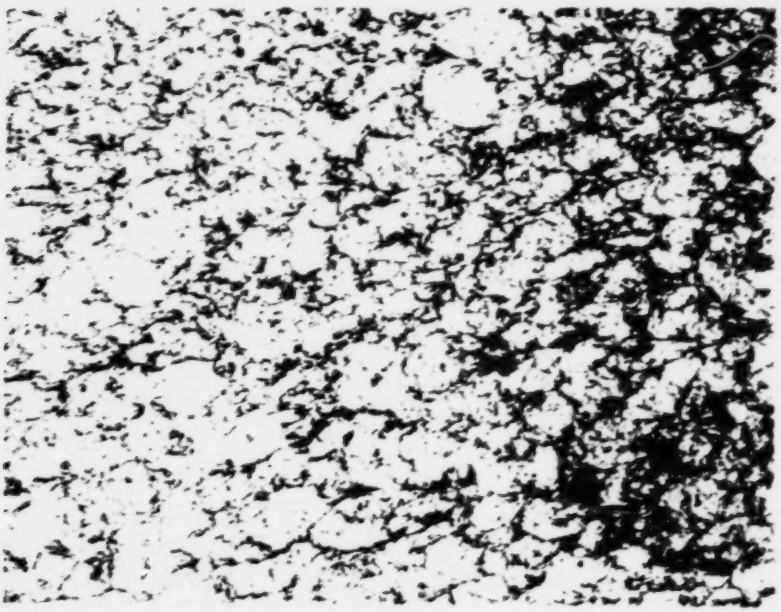

FIGURE 6a: Microstructure of R = 3.8 (top).
MAG.: X 100.

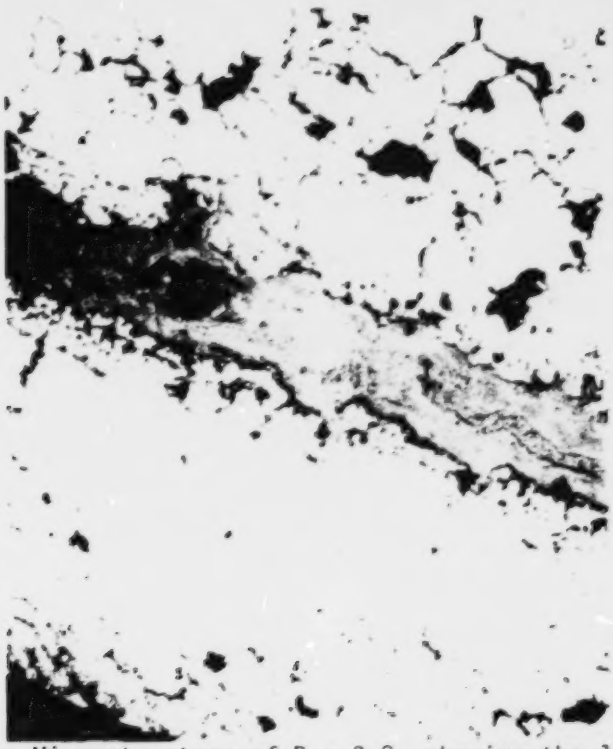

FIGURE 6b: Microstructure of R = 3.8, showing the layered structur around the mandrel. Top is the outside layer, bottom is the inside layer.
MAG.: X 100.

FIGURE 7: Unetched surface of the iron sample compacted at R = 5.2.
MAG.: X 125.

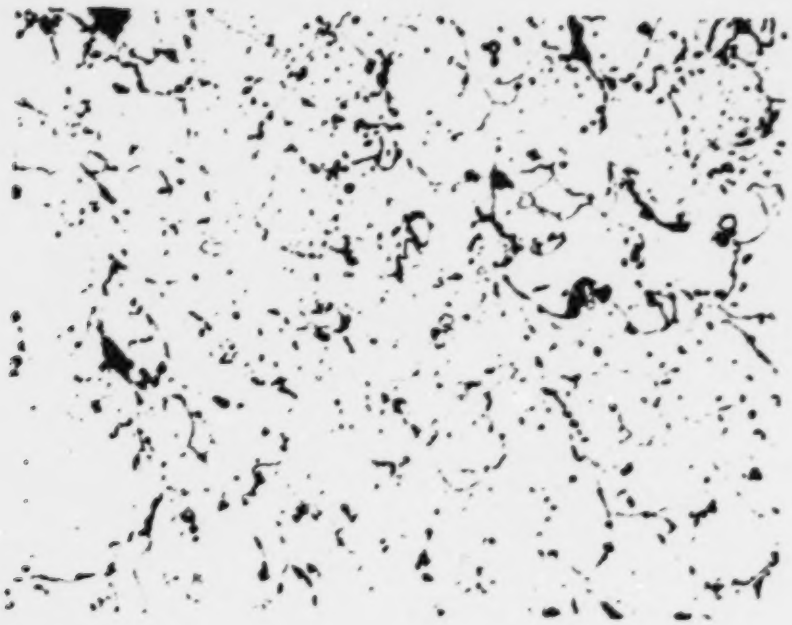

FIGURE 7a: Microstructure of R = 5.2 (top).
MAG.: X 250.

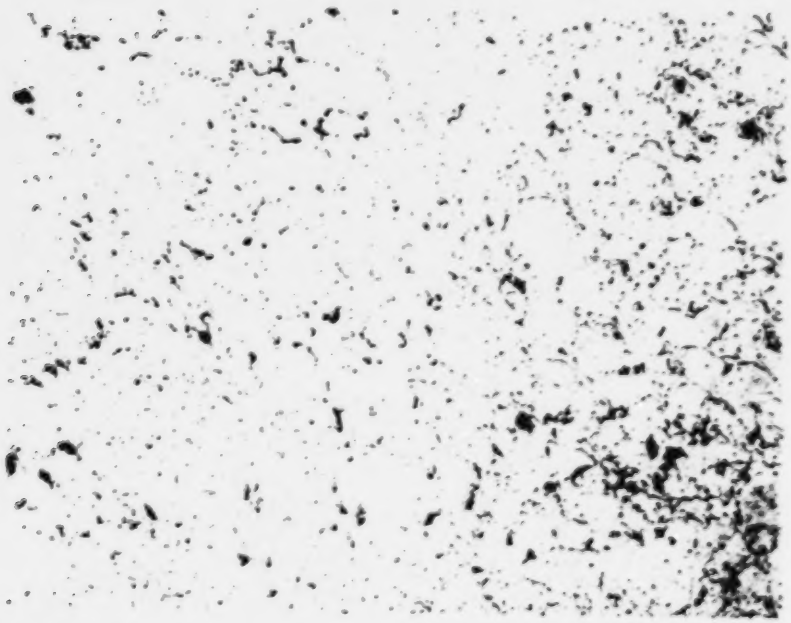

FIGURE 7b: Microstructure of R =5.2 (inner layer).
MAG.: X 100.

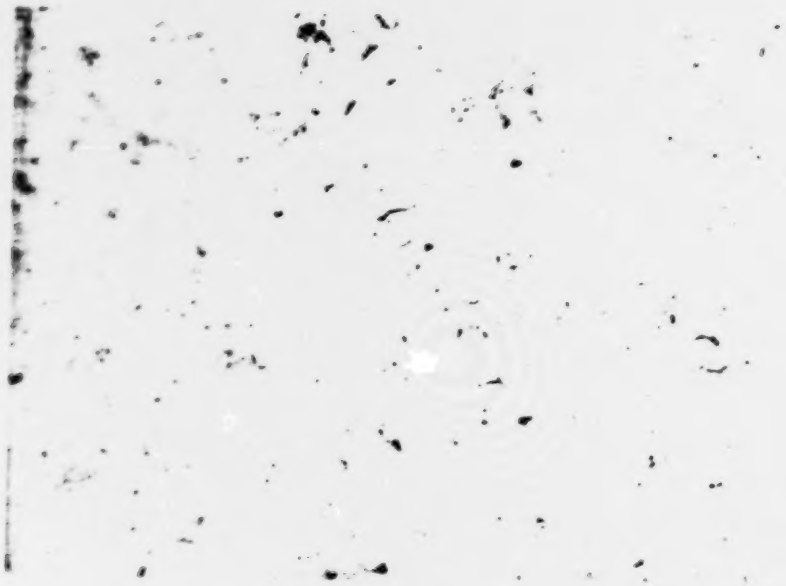

FIGURE 8: Unetched surface of the nickel-aluminium-bronze sample compacted at R = 2.8 (top).
MAG.: X 250.

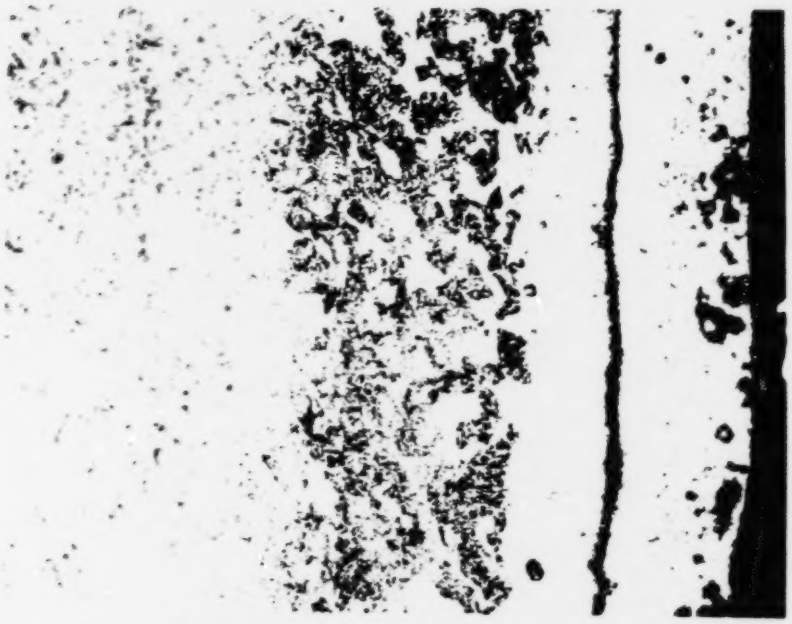

FIGURE 8a: Microstructure showing the different phases of the nickel-aluminium-bronze sample, R = 2.8.
Left (outer phase), right (inner phase).
MAG.: X 250.

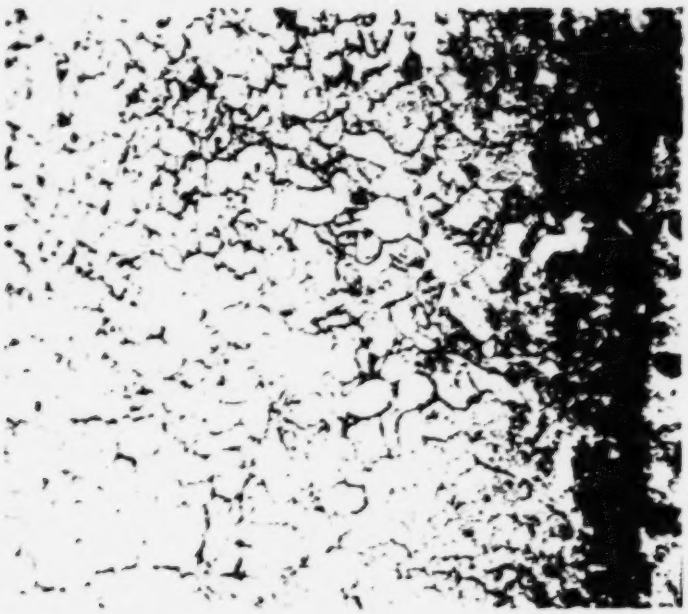

FIGURE 8b: Microstructure of a section taken from around the mandr
of R = 2.8.
MAG.: X 250.

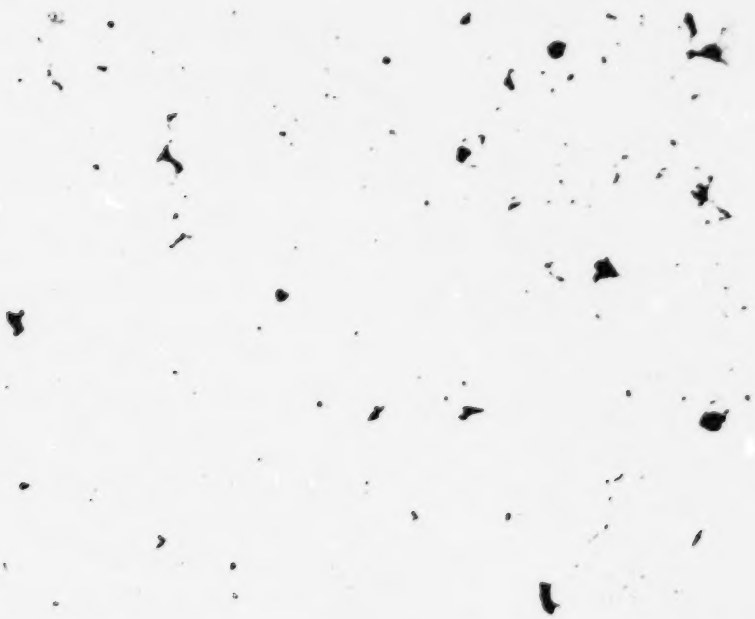

FIGURE 9: Unetched surface of the nickel-aluminium-bronze sample
compacted at R = 5.2 (top).
MAG.: X 250.

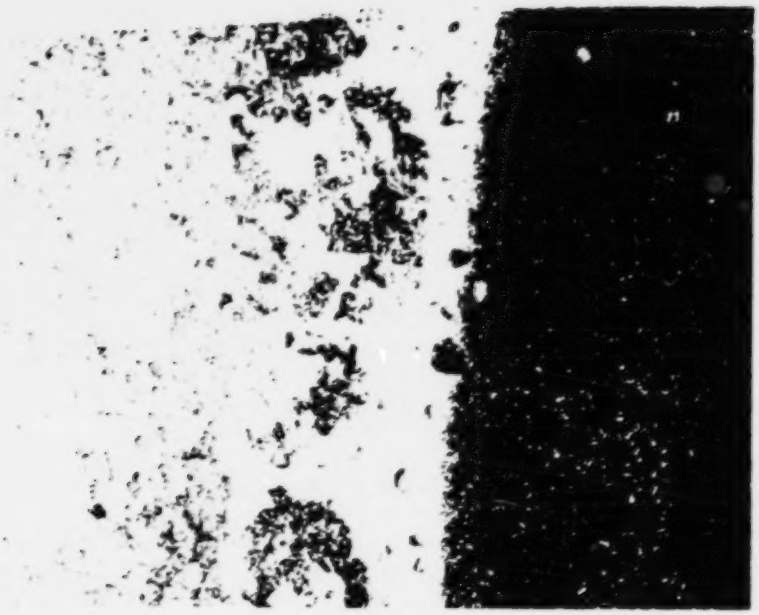

FIGURE 9a: Microstructure showing the different phases of the sample compacted at R = 5.2.
Left (outer phase), Right (inner phase).
MAG.: X 200.

FIGURE 9b: Microstructure of the outer phase of R = 5.2.
MAG.: X 250.

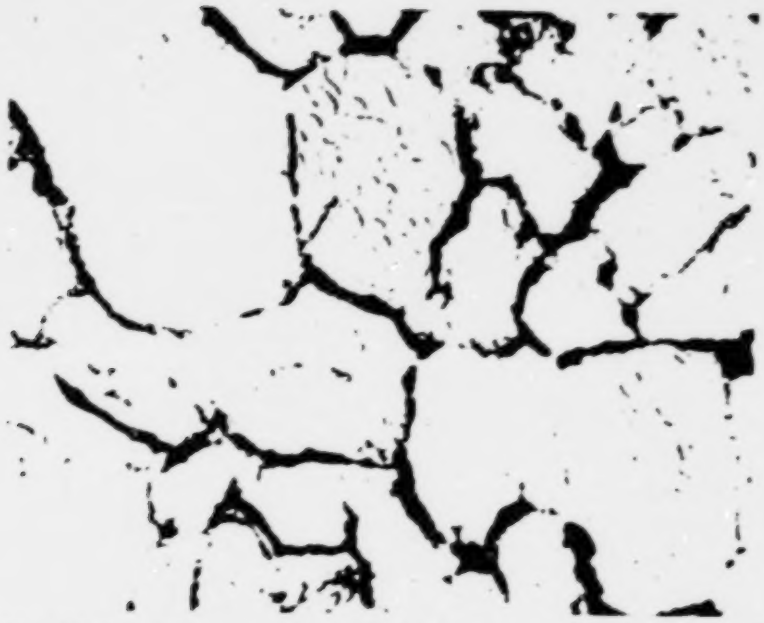

FIGURE 9c: Microstructure of the outer phase of R = 5.2 of the nickel-alumunium bronze.
MAG.: X 1600.

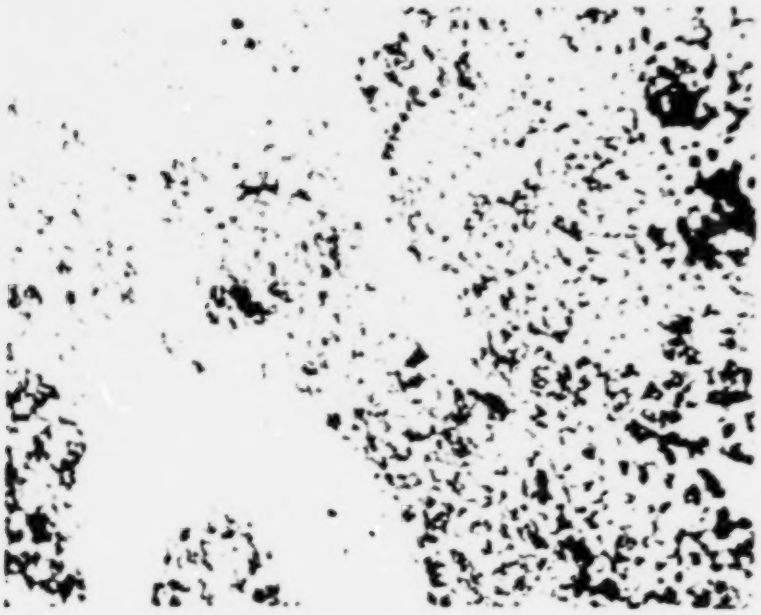

FIGURE 9d: Microstructure of the middle phase, R=5.2.
MAG.: X 1600.

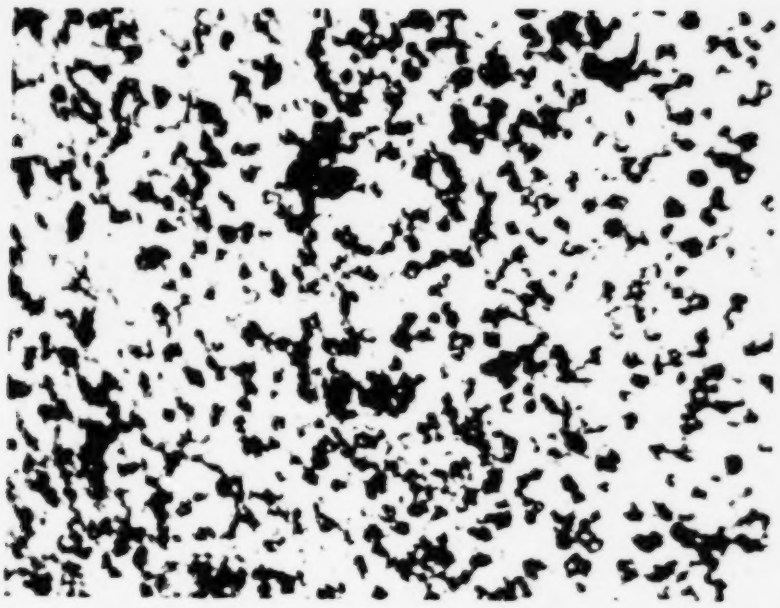

FIGURE 9e: Microstructure of the inner phase, R = 5.2.
MAG.: X 2000.

Figure 10

The Effect of Varying Charge Size Ratio (R) with an Initial Powder Density of 59.6% of Theoretical

Initial Iron Powder Density - 59.6%

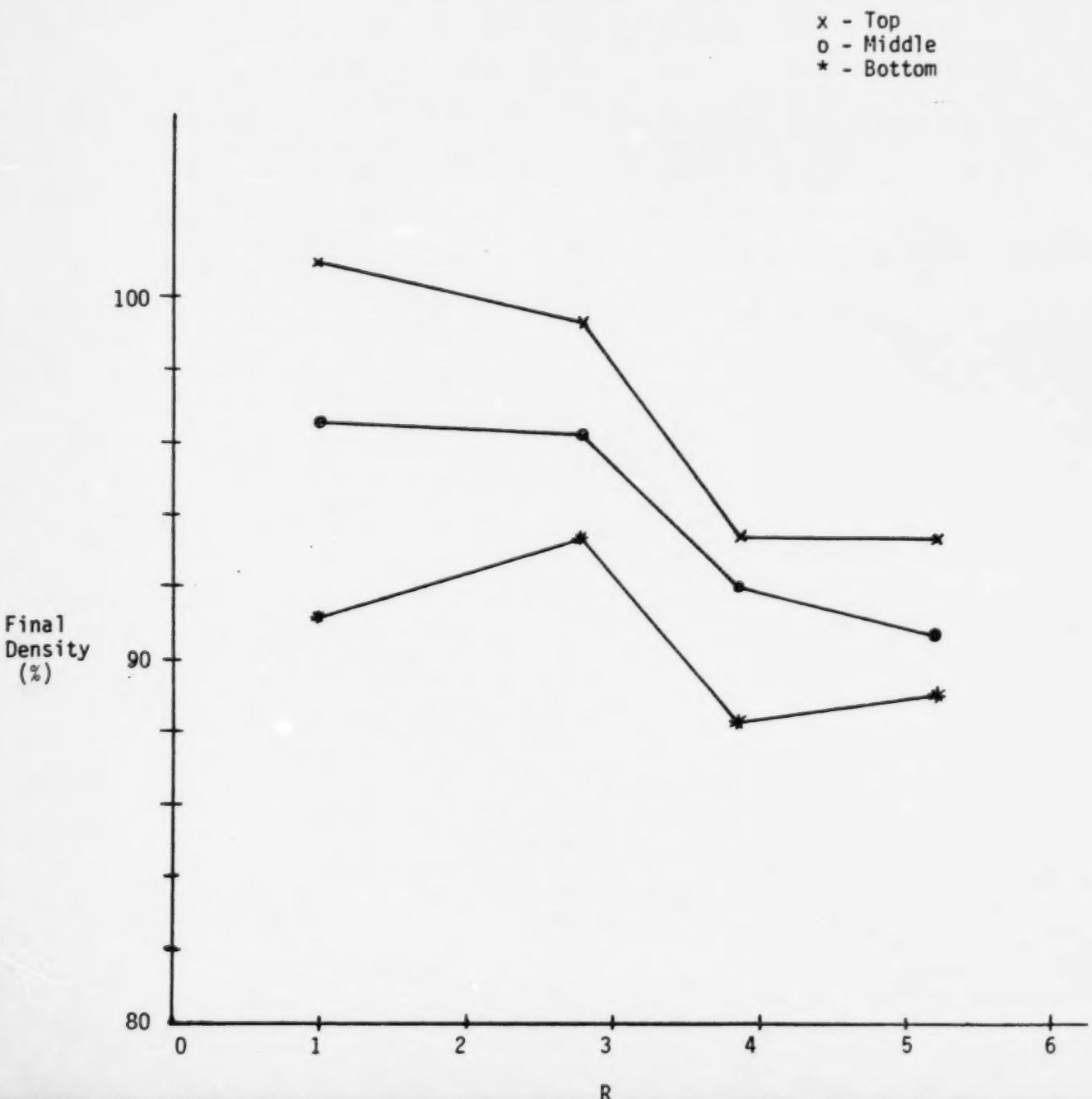

APPENDIX A: Shock Waves

SHOCK WAVE

A shock wave passing through a sample causes what might be described as an instantaneous change in state. The actual width of the shock front in a powder sample is approximately the size of a powder grain (1). Consider a shock wave passing at a speed v_s through a stationary sample of initial density d_o, initial pressure P_o and initial energy E_o. The final particle speed is v_p (the speed of the bulk motion of the compact), the final density is d, the final pressure is P and the final energy is E (see Figure 1). The equations relating these quantities before and after the shock wave are called the Rankine-Hugoniot equations (2). The equation governing conservation of mass is:

$$d_o v_s = d (v_s - v_p); \tag{1}$$

that governing transfer of momentum is:

$$P - P_o = d_o v_s v_p; \tag{2}$$

and that governing transfer of energy is:

$$E - E_o = \frac{P_o v_p}{d_o v_s} + \frac{v^2_p}{2}. \tag{3}$$

Eliminating v_s and v_p from the above equations results in the Hugoniot energy equation:

$$E_o - E = \frac{(P + P_0)}{2}\left[\frac{1}{d_o} - \frac{1}{d}\right] \qquad (4)$$

which is often written:

$$E_o - E = \frac{(P + P_0)(V_o - V)}{2} \qquad (5)$$

where V, the reciprocal of d, is the specific volume. The usual experimental procedure is to measure v_s, d_o and d. With this information, v_p is calculated from (1), P is then calculated from (2), and finally E from either (3) or (4).

For a specific shock wave velocity and pressure, the final state is determined unambiguously from the initial state. Thus, equations (1) through (5) represent equations of state. The equations of state (or Hugoniots) for a number of solid materials have been measured (2), as well as those for a number of porous samples (2,3,4,5). Hugoniots are shown schematically in Figure 2. Figure 2a shows a Hugoniot for a solid and Figure 2b that for a powder (or porous) sample.

The change in state which occurs on the passage of the shock wave is irreversible, since it results in the dissipation of energy. The amount of energy dissipated in the process is approximately given by the shaded regions in the curves in Figure 2 (6). The curves marked H represent Hugonoits for the particular sample being shocked, and the curves marked R represent straight lines between the state conditions immediately before and immediately after the shock wave front. These straight lines are also known as Rayleigh lines. The curve marked S in Figure 2b is the solid Hugonoit.

Above a certain compaction pressure (P_c), the powder sample will be compacted to the solid density, and the Hugonoit can be approximated by the solid Hugonoit. P_c is dependent on the material being compacted, but is not (strongly) dependent on the initial sample density. For example, copper powder is fully compacted by a shock pressure of about 21 kbar (3) and tungsten by about 45 kbar (5).

SHOCK WAVE SOURCES

Shock waves are usually generated by impacting a sample with a high speed projectile or with an explosion. Each of these methods has advantages and disadvantages.

The use of projectiles has the advantage that the energy and the momentum of the collision can be adjusted independently. This is done by changing the projectile mass and velocity. Having these degrees of freedom is very useful in controlling the compaction process. The disadvantage of using projectiles is that a gun or accelerator is necessary to impart the energy into the projectile. At the high speeds used in shock wave compaction, the guns tend to be very large and expensive (7).

Explosives are a less expensive source of shock waves than are projectiles. Explosive shock waves are, however, less well controlled than those from projectile impacts. The variables are explosive burn velocity and explosive mass (or energy). The burn velocity is determined by the explosive type and thus cannot be set at any arbitrary value. Because of the lower expense involved in explosive compaction, this is the preferred method to be used in initial compaction trials.

REFERENCES

(1) W. H. Gourdin, J. Appl. Phys., 55, 1984, pp 172-180.

(2) R. G. McQueen, S. P. Marsh, J. W. Taylor, J. N. Frite and W. J. Carter, in "High-Velocity Impact Phenomena", ed. by R. Kinslow, Academic Press, New York, 1970, pp 293-417.

(3) R. R. Boade, J. Appl. Phys., 39, 1968, pp 5693-5702.

(4) R. R. Boade, J. Appl. Phys., 40, 1969, pp 3781-3785.

(5) R. R. Boade, J. Appl. Phys., 41, 1970, pp 4542-4551.

(6) "Dynamic Compaction of Metal and Ceramic Powders", Report of the Committee on Dynamic Compaction of Metal and Ceramic Powders, National Academic Press, Washington, D.C., 1983.

(7) A. J. Cable, in "High-Velocity Impact Phenomena", ed. by R. Kinslow, Academic Press, New York, 1970, pp 1-21.

Figure 1

A Shock Wave Passing through an Object which is Initially at Rest

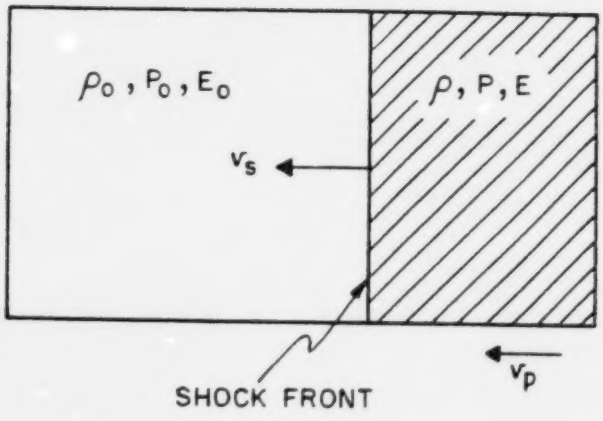

Figure 2

Hugoniots Relating Pressure and Specific Volume

Figure 2a shows the curve for a solid sample, and Figure 2b shows the curve for a powder sample made up of the same material as in 2a. Curves marked H are Hugoniots, curves marked R are Rayleigh lines, and the curve marked S represents the solid Hugoniot.

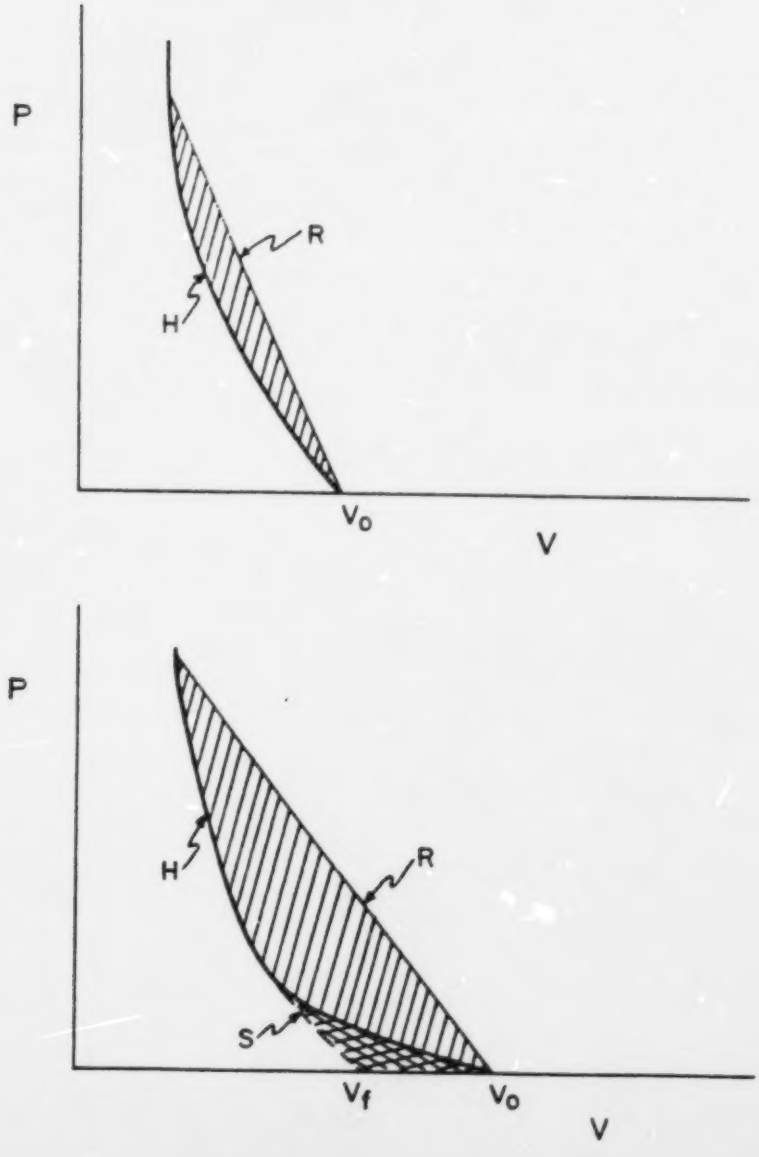

APPENDIX B: Shock Wave Compaction Geometry

Cylindrical compaction geometry was used in all the compaction trials for the iron and nickel-aluminum-bronze powders.

A schematic diagram of an assembled cylindrical compaction unit is shown in Figure 3 of the main body of this report. This diagram shows a cross-sectional view of a cylinder to be compacted. Because of the geometry of the sample, projectiles cannot be easily used and explosives are the practical method of generating the shock wave. The explosive(s) are packed around the cylindrical sample and ignited at one end. The explosive shock hits equally and at the same time around the circumference of the cylinder, and travels along the length of the cylinder.

In this compaction geometry, the compacted material is still moving with a velocity v_p, but now this material is moving towards the centre of the cylinder. There is a build-up of energy in the centre above the energy absorbing mandrel as the material from opposite sides of the cylinder collides. This results in a structurally damaged region along the middle of the sample above the mandrel. This region is called the Mach Stem (Figure 1a).

The material around the mandrel forms a compact. When the mandrel is removed, a compacted sample is left in the shape of a ring (Figure 2).

Figure 1

Cylindrical Compaction

Shaded areas are behind the shock front

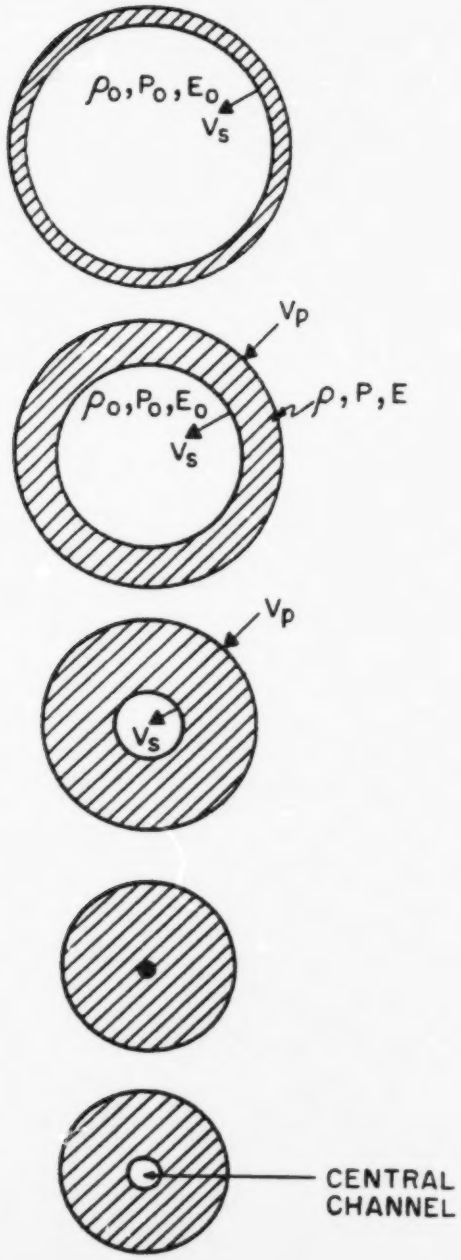

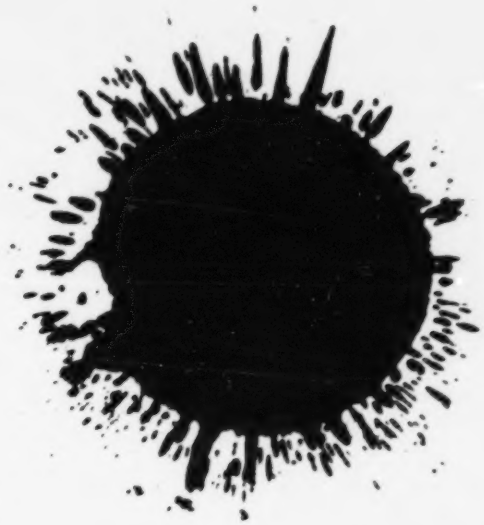

FIGURE 1a: Sectioned sample showing formation of Mach Stem.
MAG.: X 21.

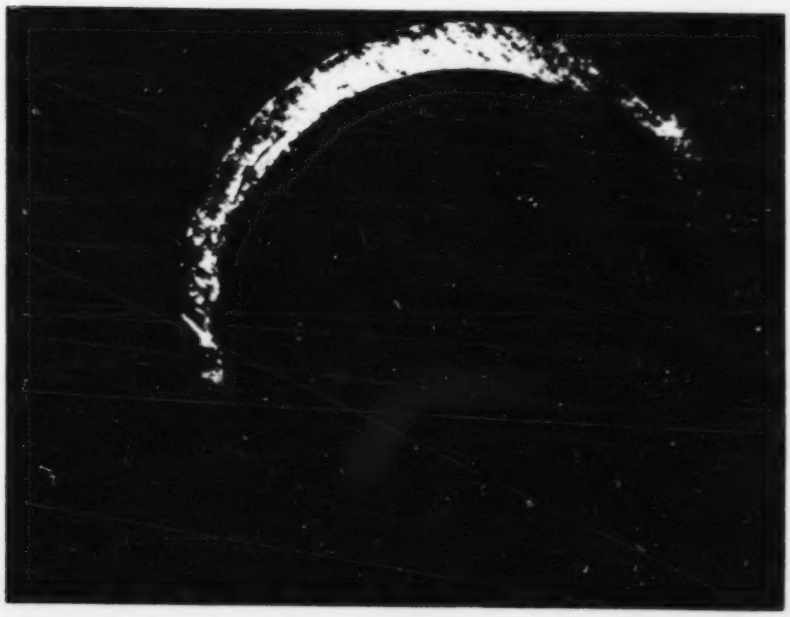

FIGURE 2: Section of a sample with the energy absorbing mandrel removed.
MAG.: X 5.

REFERENCES

(1) Raybould, Powder Metallurgy, 25, 1982, pp 35-41.

(2) M. A. Meyers and B. B. Gupta, Journal of Metals, October 1981, pp 21-26.

(3) "Dynamic Compaction of Metal and Ceramic Powders", Report of the Committee on Dynamic Compaction of Metal and Ceramic Powders, National Academic Press, Washington, D.C., 1983.

APPENDIX C: Particle Surface Temperature and Compaction Rate

The energy which is used to compact a powder goes into two basic processes. One process involves compressing the powder (and thus increasing the bulk kinetic energy of the sample), and the other involves raising the temperature of the compacted specimen. If the velocity of the compaction wave is large, then most of the heating occurs at the surfaces of the particles. The particle surface temperature is given by(1):

$$T_s = T_o + \frac{E}{C_p} + \frac{v_s E \rho_o}{6K}\, d \left[0.1 - \sum_{\eta=1}^{\infty} \frac{1}{X^2_\eta} \exp\left(\frac{-4 \alpha X^2_\eta}{v_s\, d} \right) \right]$$

where T_s is the maximum surface temperature
T_o is the initial powder temperature
v_s is the speed of the compaction shock wave
E is the deposited energy per unit mass

$$d = \frac{\Delta^2}{D} \quad \text{where } \Delta = \frac{6,}{\rho_o A}$$

A is the measured surface area per unit mass of powder and D is the particle diameter.

ρ_o is the solid density
K is the thermal conductivity of the material
X_η is the nth root of the equation $\tan X_\eta = X_\eta$
α is the thermal diffusivity of the material

For most practical cases of interest, only the first term in the sum in equation 1 need be considered and, for this term, $X \approx 4.5$. In this limit, the factor in the square bracket in equation 1 will range from 0.10 (for v_s small) to 0.05 (for v_s large).

REFERENCE

(1) W. H. Gourdin, J. Appl. Phys., 55, p 172, 1984.

APPENDIX D: Calculating Effective Explosive Charge Sizes

The process of imparting energy into a work piece, through the detonation of an explosive, is complicated. An understanding of this process is hampered by the high speed at which it takes place, and by the hazardous nature of an explosive event. A number of engineering formulae are used to calculate the amount of energy transferred from an explosive to a work piece, and these formulae are discussed in this appendix. This topic is discussed in detail in the references (1, 2).

The traditional geometry considered is that of an explosive welding process, in which one of the sections to be welded is accelerated into the other. The accelerated component is called the flyer plate, and the stationary component is called the parent plate. The energy transferred to the system is the kinetic energy of the flyer plate. The quantity calculated is the velocity of the flyer plate, Vp.

The effective energy density of the explosive is designated E, and the flyer plate velocity is given by:

$$Vp = \sqrt{2E}\, f(R)$$

where R is the ratio of explosive mass to flyer mass, and f(R) is a function which depends on the geometry of the set-up. Examples of forms for f(R) can be found in equations 4.12 and 4.13 of (1).

The value of E is not simply related to the caloric energy density of the explosive. For low density explosives, the value of E is a smaller fraction of the caloric energy density than for high density explosive. Table I lists the properties of the explosive.

Rather than using equations to calculate Vp, a nomograph can be used. An example of such a nomograph for a flat geometry (taken from (2)) is shown in Figure 1. In this figure, the effective energy is plotted on the right-hand axis (in

the form $\sqrt{2E}$) and the value of R is plotted on the slanted central axis. The value of Vp is found by drawing a straight line from the appropriate point on the energy axis, through the value of R in the central axis, and onto the left-hand axis. The intercept point on the left-hand axis gives the flyer plate velocity.

Although the geometry used in this study was not flat, the results from this graph are likely a reasonable estimate of the flyer plate velocity.

TABLE I

PROPERTIES OF EXPLOSIVE

Explosive	Density (kg/m^3)	E (kJ/kg)	Caloric Energy Density (kJ/kg)
Amatol	1,600	2,000	4,100

High Energy Rate Compaction of R.S. Metal Powders
For Limpact Industries Limited

Figure 1

Nomograph for the Determination of Flyer Plate Velocity (taken from (2))

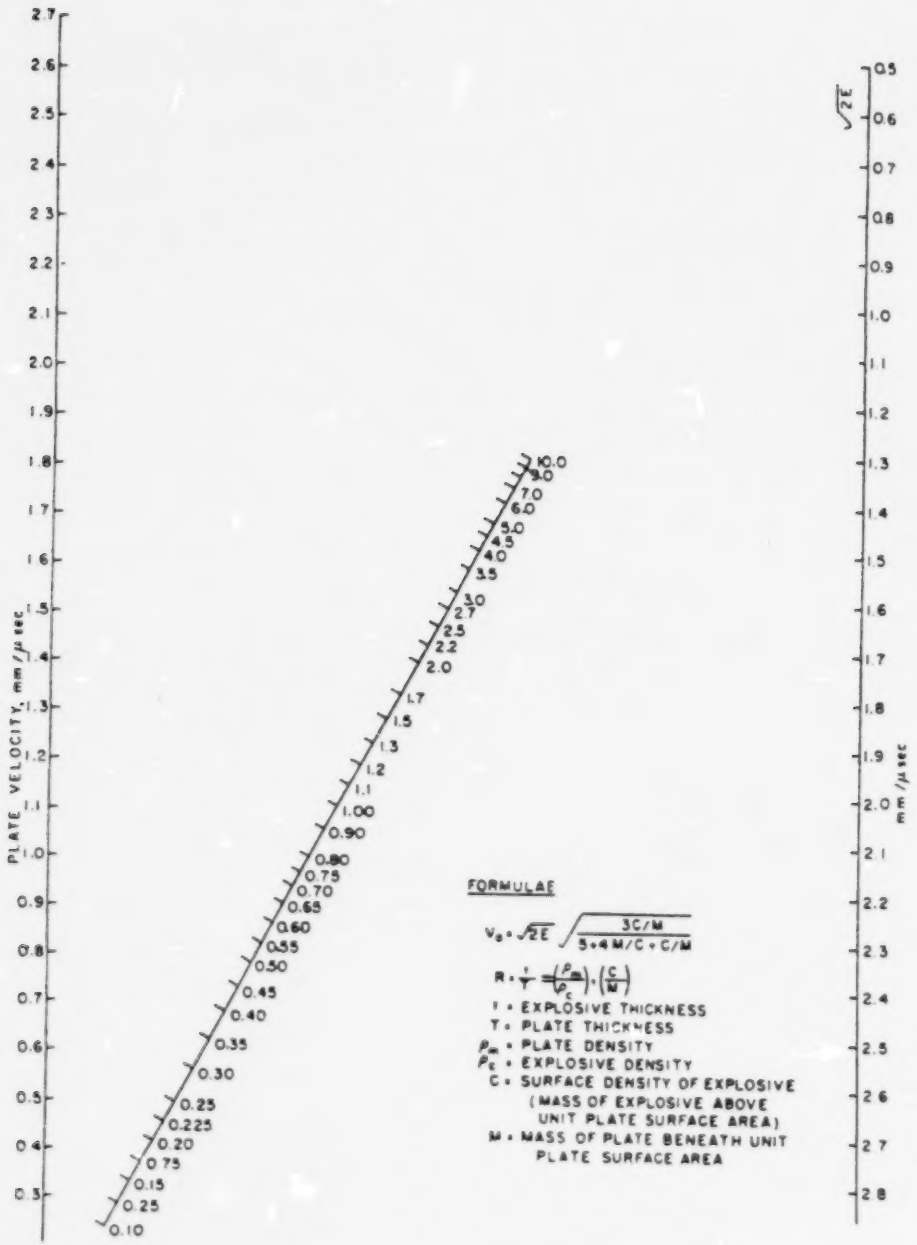
PLATE VELOCITY, mm/μ sec
√2E
E mm/μ sec
FORMULAE
$V_0 = \sqrt{2E}\sqrt{\frac{3C/M}{5+4M/C+C/M}}$
$R = \frac{I}{T} = \left(\frac{\rho_m}{\rho_c}\right)\cdot\left(\frac{C}{M}\right)$
I = EXPLOSIVE THICKNESS
T = PLATE THICKNESS
ρ_m = PLATE DENSITY
ρ_c = EXPLOSIVE DENSITY
C = SURFACE DENSITY OF EXPLOSIVE (MASS OF EXPLOSIVE ABOVE UNIT PLATE SURFACE AREA)
M = MASS OF PLATE BENEATH UNIT PLATE SURFACE AREA

REFERENCES

(1) B. Crossland, "Explosive Welding of Metals and its Application", Clarendon Press, Oxford, 1985.

(2) M. A. Meyers, L. E. Murr, "Shock Waves and High-Strain-Rate Phenomena in Metals", Plenum Press, New York, 1981.